https://doi.org/10.48048/tis.2023.6521

Effect of Annealing on the Structural and Optical Properties of ZnO/ITO and AZO/ITO Thin Films Prepared by Sol-Gel Spin Coating

Paulus Lobo Gareso[1,*], Heryanto Heryanto[1], Eko Juarlin[1] and Paulina Taba[2]

[1]Department of Physics, Faculty of Mathematics and Natural Sciences, Hasanuddin University, Makassar 90245, Indonesia
[2]Department of Chemistry, Faculty of Mathematics and Natural Sciences, Hasanuddin University, Makassar 90245, Indonesia

([*]Corresponding author's e-mail: pgareso@fmipa.unhas.ac.id)

Received: 14 September 2021, Revised: 6 November 2021, Accepted: 13 November 2021, Published: 27 December 2022

Abstract

This paper aims to investigate the effect of annealing on the structural and optical properties of ZnO/ITO and AZO/ITO thin films. In the preparation of ZnO and AZO films, zinc acetate dehydrate ($Zn(CH_3COO)_2.2H_2O$), ethanol, diethanolamine (DEA), and $AlCl_3$ were used as a starting material, solvent, stabilizer, and dopant sources, respectively. Both ZnO and AZO films were fabricated on ITO (indium tin oxide) substrates using the spin coating technique at room temperature with a rotating speed of 3,000 rpm in 30 s. The films were heated at various temperatures in the temperature range of 400 - 600 °C for 60 min. The crystallite size of the film is calculated using Debye-Scherrer and Williamson-Hall Methods. Based on the UDM results, the crystallite size of ZnO/ITO and AZO/ITO films increases after annealing in comparison with the films before annealing. From the optical UV-Vis measurements, there was an increase in the transmittance value of the samples after annealing. The transmittance value of ZnO/ITO and AZO/ITO films increases from 40 % before annealing to approximately 80 and 90 %, respectively after annealing. The increase in the transmittance valued in both ZnO/ITO and AZO/ITO after annealing is mainly due to an improvement in the crystalline phase of these films. The band gap energy of ZnO and AZO films is reduced with increasing annealing temperatures, from 3.26 eV before annealing to 3.19 eV for ZnO and 3.23 eV for AZO films after annealing at 600 °C.

Keywords: AZO thin films, Excitonic absorption, Refractive index, Spin coating, Thermal annealing

Abbreviations

$AlCl_3$	Aluminum trichloride
AZO	Aluminum zinc oxide
GaN	Gallium nitride
ITO	Indium tin oxide
JCPDS	Joint Committee on Powder Diffraction Standards
LED	Light-emitting diode
UDM	Uniform deformation method
UV-Vis	Ultraviolet-visible
ZnO	Zinc oxide

Introduction

Zinc oxide (ZnO) is one of the most important groups II-VI semiconductors and has been received considerable attention from many researchers to investigate it due to its electrical and optical properties. At room temperature, ZnO has a band gap energy of 3.3 eV [1-3], and it has a large exciton binding energy of 60 meV [4,5]. These features make ZnO applicable in LED [6], photovoltaic devices [7], and electrochemical sensors [8]. In addition, the visible region of a ZnO thin film used as a solar window has a high optical transmittance [9]. Moreover, ZnO has band gap energy and optical properties identical to GaN materials, which is good for fabricating optical devices such as laser diodes (LDs) [10].

Various methods have been applied to fabricate ZnO thin film, such as; RF magnetron sputtering [11], molecular beam epitaxy (MBE) [12], spray pyrolysis [13], pulsed laser deposition (PLD) [14], electrodeposition [15], and sol-gel spin coating method [16-18]. Among other techniques, the sol-gel spin coating is one of the attractive techniques to fabricate thin films due to its simplicity, the inexpensive cost

to characterize the structural and optical properties, and the ease of controlling chemical compounds. Many researchers have extensively reported the fabrication of the ZnO films on different substrates such as glass, silicon, and quartz [19-22]. However, to the best of our knowledge, the deposition of ZnO films on ITO substrate using spin coating approach has not received much attention for researchers to investigate it [23]. The growth of ZnO films on ITO substrates can increase the films' resistance, thereby improving the electrical and optical properties of the films and improving the device performance [24,25].

In this present study, we investigate the effect of annealing on the structural and optical properties of ZnO/ITO and AZO/ITO films using the sol-gel spin coating method. The use of the aluminum atom as a dopant in this work is motivated by the higher value of conductivity and better transparency than other dopants such as Fe, Ga, and Sn [26]. For these purposes, ZnO and AZO films were coated by sol-gel spin coating technique on ITO substrates, and they were annealed at different temperatures from 400 - 600 °C for 60 min.

Materials and methods

The ZnO and AZO thin films were prepared by zinc acetate dehydrate ($Zn(CH_3COO)_2.2H_2O$) dissolved in 25 mL ethanol and 2.5 mL diethanolamine (DEA) as a solvent and stabilizer, respectively. 6.67 g of $AlCl_3$ solution was used as a dopant material dissolved in 100 mL of H_2O. The dopant solution was added to the mixture with the ratio of dopant 1 % to Zn. The mixture solution was stirred at the magnetic hotplate for 30 min at the temperature of 80 °C. Before the fabrication of ZnO and AZO films, the ITO substrates were cleaned in methanol and acetone for 10 min each by an ultrasonic cleaner, washed with de-ionized water, and dried. The sol-gel solutions were deposited on the ITO substrates using a spin coating method with a rotation speed of 3,000 rpm in 30 s. After fabrications, the films were heated at 100 °C for 15 min at a rapid thermal processor (RTP) to evaporate the solvent and remove the unwanted organic residuals. Next, the films were inserted into the tube furnace and annealed at different temperatures at 400 - 600 °C for 60 min. **Figure 1** displays the procedure for fabricating the ZnO and AZO thin films on ITO substrates.

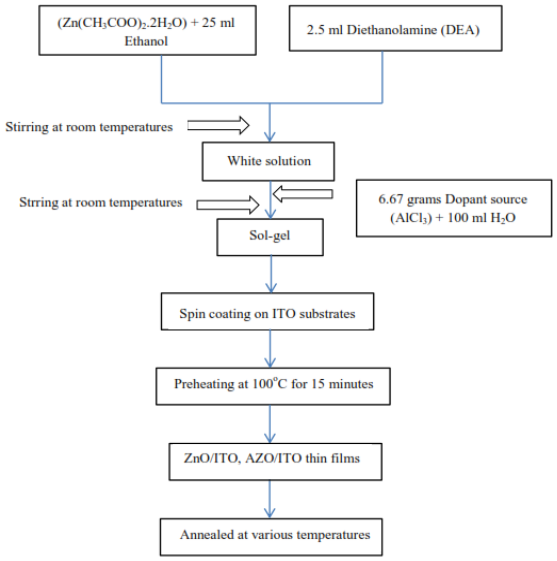

Figure 1 The flowchart scheme of the sol-gel spin coating process for the preparation of ZnO and AZO thin films on the ITO substrates.

The structural properties of the films were characterized by X-ray diffraction (XRD) measurements (Shimadzu 700) using Cu Kα radiation (λ = 1.5406 Å) with the scanning diffraction angle range of 20 - 70 °. During the measurements, the current and the voltage of X-RD were constant at 30 mA and 40 kV, respectively, with the scan speed of XRD being 2 °/min. From the X-RD results, the Debye-Scherrer equation and Williamson-Hall method were used to estimate the crystallite size of the films. The UV-Vis Optical transmittance measurement was carried out to characterize the optical properties using a single beam UV-Vis spectrophotometer (Shimadzu UV-Vis Spectrophotometer 1800) with a wavelength range of 250 - 800 nm.

Results and discussion

Figure 2(a) displays the X-ray diffraction curves of the ITO substrates before ZnO, and AZO films were deposited on it. The XRD spectra appeared at diffraction angles of 44.4 and 65.8 ° that corresponded to (102) and (200) planes, respectively (JCPDS card no: 96-900-8571 and 96-101-0943). **Figure 1(b)** shows the XRD curves of ZnO/ITO films before and after annealing at various temperatures ranging from 400 - 600 °C for 60 min. As shown in **Figure 2(b)**, the XRD curves of ZnO films were not observed before annealing the films. The XRD peaks that emerged in this film originated from the ITO substrates (see **Figure 1(a)**). This result was probably due to amorphous ZnO films, which could not provide an adequate diffracted intensity. However, the additional peaks were observed in the XRD curves after annealing the films at 400 °C, corresponding to ZnO films. In addition to this, more peaks of ZnO films were detected after annealing the films at 500 and 600 °C. Interestingly, the (002) plane was not seen in ZnO films after annealing at 400 °C. However, this plane was observed after annealing at 500 and 600 °C. Previous studies confirmed our results where the peak intensity of ZnO films increased significantly after annealing at high temperatures compared with low annealing temperatures. The increase of the peak intensity was due to the improvement in the crystallinity of the films after annealing [26]. Also, it is demonstrated in **Figure 1(b)** that after annealing the films at 500 and 600 °C, ZnO films showed polycrystalline with hexagonal wurtzite crystal structures, which have the preferential orientation of (100) plane.

The XRD curves of the AZO/ITO films before and after annealing at various temperatures ranging from 400 - 600 °C for 60 min are depicted in **Figure 3**. As shown in this figure, there was no peak corresponding to the AZO films detected before annealing. However, the XRD curves of the AZO films were seen after annealing the films at 400, 500 and 600 °C, respectively. As shown in the **Figure 2**, no peak was detected for (002) plane in AZO films after annealing. Also, after annealing the films, the intensity of (100) peak was relatively higher than that of other peaks. It means that the preferential orientation plane of AZO films was in (100) reflection plane. Previous studies reported that the XRD peak intensity of (001) reflection plane of AZO films was higher than that of other planes indicating that the preferential orientation of AZO was in (100) plane [27]. From the XRD results, the crystallite size (D) of both ZnO and AZO thin films can be calculated using the Debye-Scherrer formulation [28].

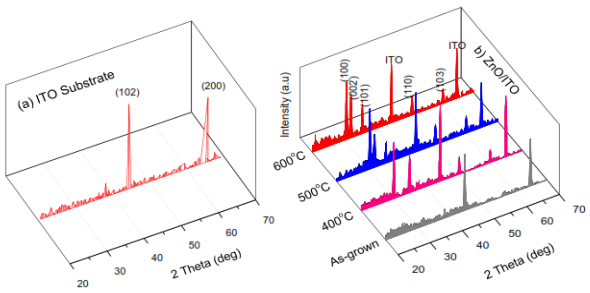

Figure 2 (a) XRD curves of ITO substrates (b) XRD curves of ZnO/ITO films before and after annealing at various temperatures from 400 - 600 °C for 60 min.

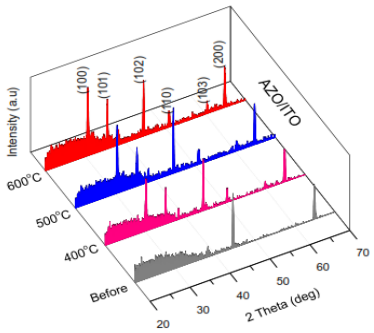

Figure 3 XRD curves of AZO/ITO films before and after annealing at various temperatures from 400 - 600 °C for 60 min.

$$D = \frac{k\lambda}{\beta_D cos\theta} \quad (1)$$

where k is a constant equal 0.9, λ is the X-ray wavelength (λ = 1.5406 Å), β_D is the full width at half-maximum (FWHM), and θ is the Bragg angle, respectively. From Eq. (1), after annealing at 400 °C, the average crystallite size of ZnO films was around 38.75 nm, and it increased to 52.02 nm after annealing at 600 °C. For the case of AZO films, the average crystallite size of this film increased from 33.35 nm after annealing at 400 °C - 35.58 nm at 500 °C annealing (see **Table 1(a) - 1(b)**). The average crystallite size of the films was determined based on **Figures 2** and **3**, which have a high intensity in the plane structures of XRD curves. It means that the plane structures with small intensity were not considered in determining the films' average crystallite size. Also, the Williamson-Hall method (Uniform Deformation Method=UDM) was used to calculate the crystallite size and the strain of both ZnO and AZO films. In this method, the crystallite size and the strain are 2 components that contributed to the peak broadening. Taking the Scherrer equation and the strain $\varepsilon=\beta_s/4\tan\theta$ result in the following equation [29,30].

$$\beta_{hkl} = \beta_D + B_S \quad (2)$$

$$\beta_{hkl} = \frac{k\lambda}{D\ cos\theta} + 4\varepsilon tan\theta \quad (3)$$

Rearranging Eq. (2) gives:

$$\beta_{hkl} cos\theta = \frac{k\alpha}{D} + (4\varepsilon\ sin\theta) \quad (4)$$

The Eq. (4) represents UDM, where it is assumed that the strain is uniform in all crystalline directions, in which the properties of the materials are independent [29,30]. The term β_{hkl} cosθ, when plotted against 4sinθ would give the slope and *y*-intercept of the fitted line representing the strain and the crystallite size of the samples, respectively. **Figures 4** and **5** depict the Williamson-Hall method of analyzing ZnO/ITO and AZO/ITO films. Based on these figures, the strain was negative in both ZnO/ITO and AZO/ITO, indicating that the strain of the films might be due to the shrinkage of the lattice parameters of the films. The crystallite size of the ZnO increased from 29.58 nm after annealing at 400 °C - 41.41 nm annealing at 600 °C. The crystallite size rises from 34.31 nm (400 °C) to 36.19 nm (600 °C) for AZO films. The crystallite size of AZO/ITO films derived from UDM is almost similar to Debye Scherrer, it is approximately 1.019 times larger than Debye-Sherrer. In addition, both the Debye-Scherrer and Williamson-Hall method (UDM) showed an increase in the crystallite size of ZnO and AZO films after annealing at high temperatures compared to low-temperature annealing. A previous study has reported that the crystallite size of ZnO and AZO films increased with the annealing temperatures. They revealed that as the annealing increased, the crystallite size increased, followed by increasing the intensity indicating the improvement of the crystalline of the films during the annealing [31].

Table 1 (a) The structure parameters of ZnO/ITO films after annealing at various temperatures in the range of 400 - 600 °C for 60 min and (b) The structure parameters of AZO/ITO films after annealing at various temperatures in the range of 400 - 600 °C for 60 min.

Annealed samples	2θ	(hkl)	Scherer method [28]		Williamson hall plot method [29,30] Uniform deformation method (UDM)	
			Size (nm)	Average size (nm)	Size (nm)	Strain ($\times10^{-3}$)
400 °C	30.11	(100)	37.39	38.75	29.58	1.50
	34.79	(002)	62.16			
	35.01	(101)	40.11			
	50.02	(110)	65.45			
	61.34	(103)	74.27			
500 °C	30.27	(100)	46.33	41.31	39.17	0.63
	34.56	(002)	86.97			
	35.17	(101)	36.30			
	50.63	(110)	45.90			
	61.87	(103)	69.10			

Annealed samples	2θ	(hkl)	Scherer method [28]		Williamson hall plot method [29,30] Uniform deformation method (UDM)	
			Size (nm)	Average size (nm)	Size (nm)	Strain ($\times 10^{-3}$)
	30.58	(100)	46.79			
	35.02	(002)	60.08			
	36.23	(101)	49.19			
600 °C	50.50	(110)	73.23	52.02	41.41	0.12
	61.69	(103)	58.02			
	30.19	(100)	31.86			
	34.58	(002)	62.12			
	35.11	(101)	34.84			
400°C	50.46	(110)	34.00	33.35	34.31	0.52
	60.56	(103)	48.08			
	30.46	(100)	33.45			
	34.43	(002)	79.03			
	35.40	(101)	37.09			
500°C	50.93	(110)	38.12	35.27	35.62	0.18
	60.70	(103)	60.14			
	30.55	(100)	35.32			
	34.27	(002)	96.55			
	35.47	(101)	35.83			
600°C	50.87	(110)	26.27	35.58	36.19	0.12
	60.43	(103)	45.76			

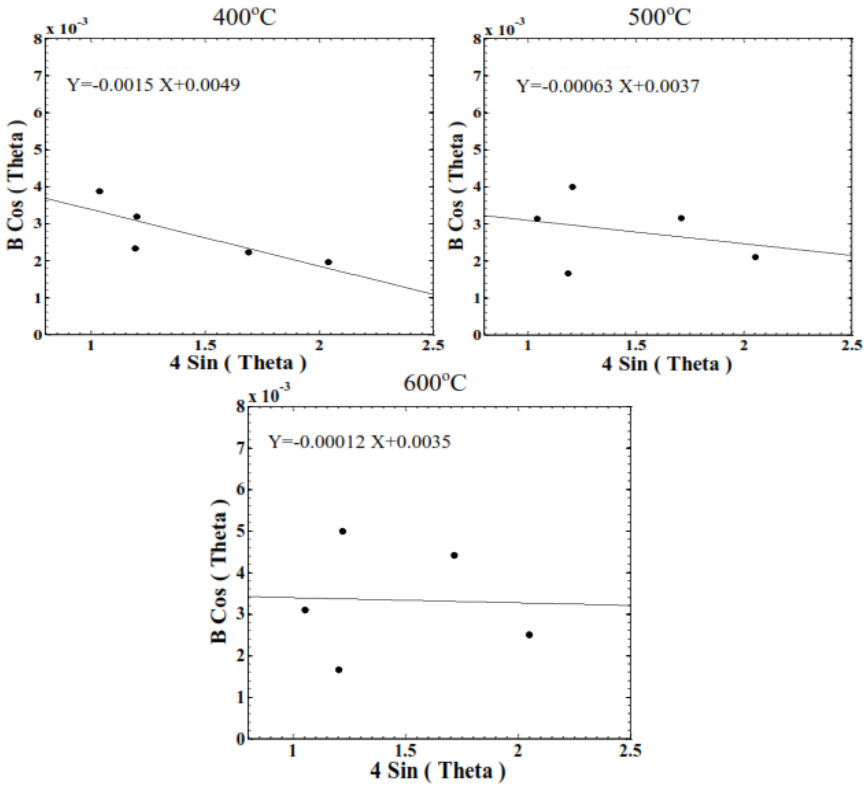

Figure 4 The Williamson-Hall analysis of undoped ZnO after annealing at various temperatures of 400, 500 and 600 °C, respectively assuming UDM. The crystallite size and the strain are extracted from the y-intercept and the fit slope, respectively.

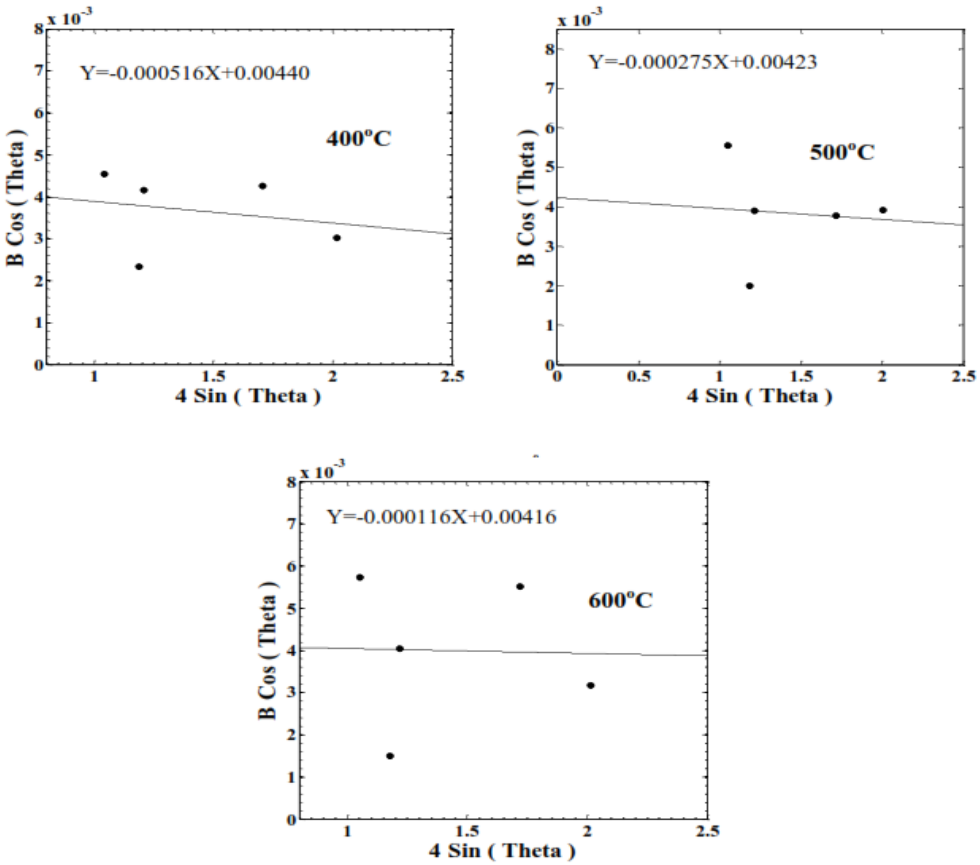

Figure 5 The Williamson-Hall analysis of AZO thin films after annealing at various temperatures of 400, 500 and 600 °C, respectively assuming UDM. The crystallite size and the strain are extracted from the y-intercept and the fit slope, respectively.

Figure 6(a) presents the optical transmittance and reflectance spectra (inset **figure 5(a)**) of ZnO/ITO thin films before and after annealing at various temperatures ranging from 400 - 600 °C for 60 min. As shown in this figure, the transmittance value was significantly affected by the annealing temperature. The annealing temperature increases the transmittance value from around 40 % (before annealing) to approximately 80 % after annealing at 600 °C. The rise in the transmittance value is attributed to the good crystalline, as shown in the X-RD results. Also, the transmittance spectra of ZnO/ITO reveal some excitonic absorption features depending on the annealing temperatures. No excitonic absorption was observed before annealing the ZnO films. However, annealing the films at 400, 500 and 600 °C shows the excitonic absorption peak at 361, 365 and 368 nm. These absorption peaks are very close to the excitonic bulk of the ZnO, which is located at 373 nm [32].

Figure 6(b) depicts the optical transmittance and reflectance spectra (inset **Figure 5(b)**) of AZO/ITO films before and after annealing at various temperatures ranging from 400 - 600 °C for 60 min. Similar optical characteristics of ZnO/ITO were observed in AZO/ITO thin films after annealing, in which transmittance value is influenced by annealing. Before annealing, the transmittance value of AZO/ITO thin films was around 40 %. After annealing, the transmittance value increased to approximately 90 % in the 400 - 700 nm wavelength range. Also, similar excitonic absorption features of ZnO/ITO were observed in AZO/ITO. The excitonic absorption of AZO/ITO appears at 356, 359 and 362 nm after annealing at 400, 500, and 600 °C. The excitonic absorption is usually associated with the quality and the crystal structures of the thin films in which a low density and small strain might indicate the quality of the film [33].

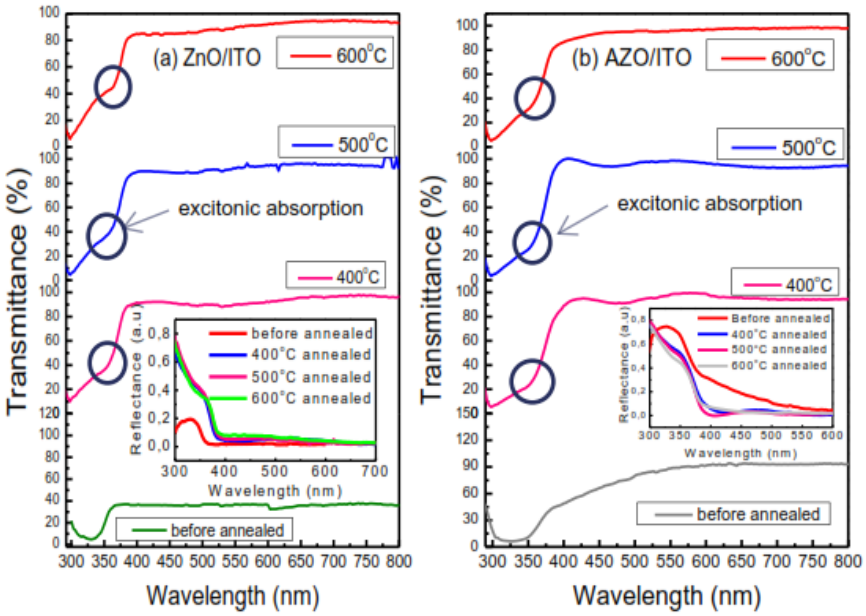

Figure 6 (a) The optical transmittance and reflectance spectra (inset figure) of ZnO/ITO film before and after annealing at various temperatures ranging from 400 - 600 °C for 60 min. (b) The optical transmittance and reflectance spectra (inset figure) of AZO/ITO film before and after annealing at various temperatures ranging from 400 - 600 °C for 60 min. Note: An oval symbol indicates excitonic absorption.

The corresponding optical band gap energy of ZnO/ITO and AZO/ITO films was estimated by extrapolating the linear relationship between $(\alpha h\upsilon)^2$ and hυ according to the equation [34].

$$(\alpha h\upsilon)^2 = A\left(h\upsilon - E_g\right) \quad (5)$$

where α is the absorption coefficient, hυ is the photon energy, E_g is the optical band gap, and A is a constant. The optical band gap value of ZnO/ITO and AZO/ITO film is determined using this equation. **Figure 7** depicts the plot of $(\alpha h\upsilon)^2$ as a function of photon energy (hυ) for ZnO/ITO and AZO/ITO thin films after annealing at different annealing temperatures ranging from 400 - 600 °C in 60 min. The optical band gap of ZnO/ITO and AZO/ITO films was estimated by extrapolating the linear portion of $(\alpha h\upsilon)^2$ against (hυ). Before annealing, the value of the band gap energy of the ZnO/ITO films was estimated to be 3.41 eV. After annealing the samples at 400, 500 and 600 °C, the band gap energy was 3.26, 3.22 and 3.19 eV, respectively. In the case of AZO/ITO films, before annealing, the estimation of the band gap energy was 3.29 eV and it was slightly reduced after annealing to 3.26, 3.24 and 3.23 eV, respectively. These results showed that the optical band gap slightly decreased with the annealing temperature in both ZnO/ITO and AZO/ITO films. Previous studies well confirm these results. Earlier studies on ZnO and AZO films confirmed our results that the band gap energy reduced with an increase in the annealing temperatures. Saleem *et al*. reported the narrowing of the band gap energy after annealing the films. The band gap energy decreases from 3.31 eV after annealing at 350 °C to 3.29 eV after annealing at 600 °C [35]. They showed that the reduction of the band gap energy of ZnO thin film as the temperatures increased was due to the increase in the crystallite size and decrease in the amorphous phase amount of the ZnO thin films. Also, Sabee *et al*. demonstrated that the band gap energy decreased with increasing the annealing temperatures. The shift of the band gap energy is probably due to reducing defects of the films with the annealing temperatures [31]. In our case, the results indicate that increasing the crystallite size and reducing the film's strain might be attributed to decreasing the film's band gap energy, as confirmed from the X-RD results. Furthermore, increasing the annealing temperature will reduce the amorphous phase since more power is supplied for crystallite growth, as a result, the improvement of the crystallinity of the films was observed as shown in UV-Vis optical transmittance. Therefore it is believed that reducing the amorphous phase and the increase of the crystallite size of the films are the main reason for narrowing the band gap energy of the films.

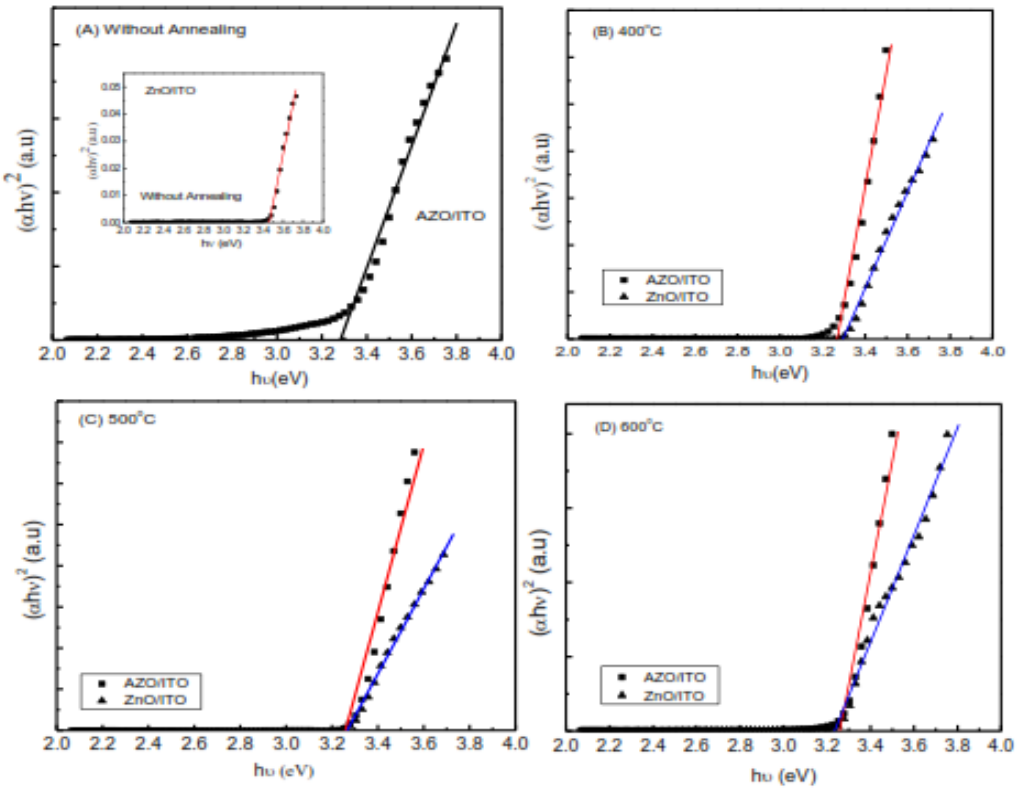

Figure 7 A plot of $(\alpha h\upsilon)^2$ vs. photon energy ($h\upsilon$) of undoped and aluminum-doped ZnO thin film before annealing (A) and after annealing at various temperatures (B) 400 °C, (C) 500 °C, and (D) 600 °C.

The refractive index (n) of ZnO/ITO and AZO/ITO films were determined using the equation below [36]:

$$n = \left(\frac{1+\sqrt{R}}{1-\sqrt{R}}\right) \quad (6)$$

where R is the reflectance of ZnO and AZO films, the value of the reflectance is derived from the transmittance as, R=1 - (T $\exp(\alpha t)^2$), where T is the transmittance, α is absorption coefficient, and t is the thickness of ZnO and AZO films. The refractive index (n) as a function of energy is displayed in the **Figure 8**. As shown in **Figure 8(a)**, the refractive index of ZnO films before annealing was around 1.25 in the energy range of 2.4 - 3.2 eV, and when the energy is up to 3.2 eV, the refractive index increased gradually. Annealing the films at 600 °C, ZnO's refractive index was around 1.75 in the range of the visible energy. The results showed that the refractive index of ZnO increased with an increase in the annealing temperatures. As a comparison in the previous study, the refractive index of ZnO film was in the range of 1.22 - 1.90. The index value of 2.0 at the photon energy of 1.96 eV was the refractive index of the ZnO single crystal. After annealing the films, the refractive index increased gradually and reached 2.35 at a photon energy of 3.2 eV [37]. In the case of the AZO films as shown in the figure.8b, before annealing, the refractive index of AZO film was larger than that of ZnO thin film, and it increased significantly. However, the refractive index of AZO films reduced in comparison to ZnO film before annealing. This value tended to be constant in the photon energy range of 2.2 - 3.0 eV, and when it was up to 3.0 eV, it increased again.

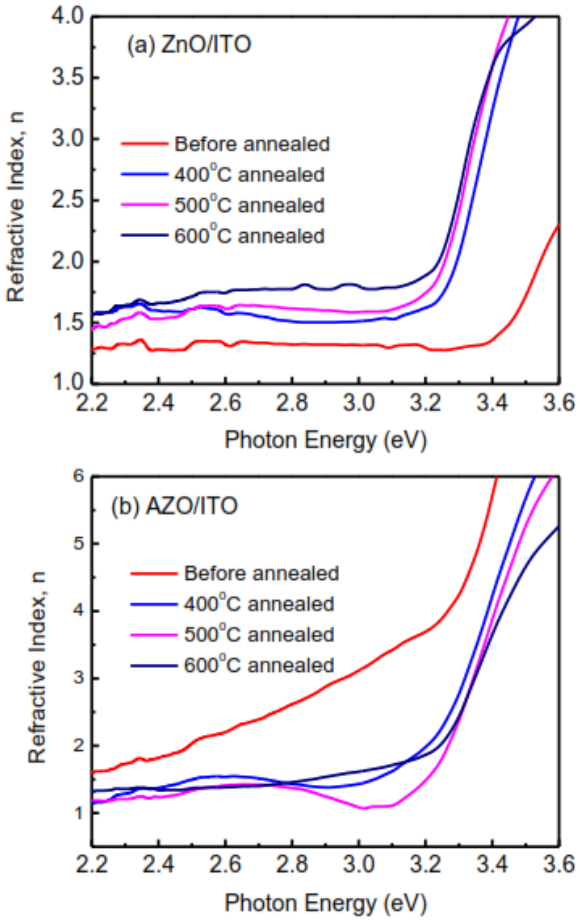

Figure 8 Refractive index of (a) ZnO/ITO, (b) AZO/ITO thin films before and after annealing at various temperatures ranging from 400 - 600 °C for 60 min.

Conclusions

The effect of annealing on the structural and optical properties of ZnO/ITO and AZO/ITO thin films has been studied using the spin coating method. Several experiments were used, such as; X-ray diffraction, scanning electron microscopy, and UV-Vis measurement. X-ray diffraction results revealed that the crystallite size of ZnO/ITO and AZO/ITO films increased with the annealing temperatures. From UV-Vis results, the transmittance value of the films was higher after annealing compared to the value before annealing. The results indicated that there was an enhancement in the crystalline phase of the films after annealing. The annealing temperatures reduced the band gap energy in both ZnO/ITO and AZO/ITO films. Reducing the band gap energy of the films after annealing is mainly due to the increase in the crystallite size of the films due to lowering the amorphous phase in the crystalline. In addition to this, the results show that the optical band gap value of AZO/ITO film was larger than that of ZnO/ITO film after annealing.

Acknowledgments

P.L. Gareso acknowledges the financial assistance from Indonesian Higher Education KEMENRISTEK-BRIN and LP2M through the research scheme of Basics Research with contract number 752/UN.4.22/PT.01.03/2021

References

[1] P Kumar, S Dev, SS Dhayal, V Acharya, S Kumar, S Kumar, N Singh and R Dhar. Synergistic effect of Mg and Se co-doping on the structural, optical and anti-bacterial activity of ZnO thin films. *Inorg. Chem. Comm.* 2021; **131**, 108801.

[2] H Guendouz, A Bouaine and N Brihi. Ultrawide bandgap high near ultraviolet transparency amorphous Sn-Al co-doped ZnO thin films. *J. Non Crystalline Solid.* 2021; **569**, 121001.

[3] A Samavati, A Awang, Z Samavati, AF Ismail, MHD Othman, M Velashjerdi, G Eisaabadi and A Rostami. Influence of ZnO nanostructure configuration on tailoring the optical bandgap: Theory and experiment. *Mater. Sci. Eng. B* 2021; **263**, 114811.

[4] YQ Su, Y Zhu, D Yong, M Chen, L Su, A Chen, Y Wu, B Pan and Z Tang. Enhanced exciton binding energy of ZnO by long-distance perturbation of doped Be atoms. *J. Phys.Chem. Lett*. 2016; **7**, 1484-9.

[5] RV Hariwal, HK Malik, A Negi and K Asokan. Favorable of optical absorbance, bandgap and surface roughness of ZnO thin films by C ion implantation at the critical angle. *Appl. Surf. Sci. Adv.* 2021; **7**, 100189.

[6] M Ding, Z Guo, L Zhou, X Fang, L Zhang, L Zeng, L Xie and H Zhao. One-dimensional zinc oxide nanomaterials for application in high-performance advanced optoelectronic devices. *Crystals* 2018; **8**, 223.

[7] J Rodrigues, AFR Cerquira, MG Sousa, NF Santos, A Pimentel, E Fortunato, AFD Cunha, T Monteiro and FM Costa. Exploring the potential of laser assisted flow deposition grown ZnO for photovoltaic applications. *Mater. Chem. Phys*. 2016; **177**, 322-9.

[8] NP Shetti, SD Bukkitgar, KR Reddy, CV Reddy and TM Aminabhavi. ZnO-based nanostructured electrodes for electrochemical sensors and biosensors in biomedical applications. *Biosens. Bioelectron.* 2019; **141**, 111417.

[9] T Logu, P Soundarrajan, D Naveena, K Sankarasubramanian, SMS Kumar and K Sethuraman. Specific Al mole ratio doping aided flake-like ZnO surface morphology nanostructures film for efficient window layer in $CuInS_2$ photovoltaic cells. *Sol. Energ.* 2019; **177**, 108-17.

[10] AM Nahhas. Review of GaN/ZnO Hybrid Structures Based Materials and Devices. *Am. J. Nano Res. Appl.* 2018; **6,** 34-53.

[11] AK Jazmati and B Abdallah. Optical and structural study of ZnO thin films deposited by RF magnetron sputtering at different thickness: A comparison with a single crystal. *Mater. Res.* 2018; **21**, 1-6.

[12] G Nam and JY Leem. Fast-response photoconductive ultraviolet light detectors fabricated using high-quality ZnO films obtained by plasma-assisted molecular beam epitaxy. *Ceram. Int.* 2017; **43**, 11981-5.

[13] S Roguai and A Djelloul. A structural and optical properties of Cu-doped ZnO films prepared by spray pyrolysis. *Appl. Phys. Mater. Sci. Process.* 2020; **126**, 122.

[14] V Kumar, SK Singh, H Sharma, S Kumar, MK Banerjee and A Vij. Investigation of structural and optical properties of ZnO thin films of different thickness grown by pulsed laser deposition method. *Phys. B Condens. Matter* 2019; **552**, 221-6.

[15] NL Okoli, CJ Nkamuo and CI Elekalachi. Effect of dip time on electrodeposited zinc oxide nanofilm. *Am. J. Mater. Synth. Process.* 2018; **3**, 7-11.

[16] A Sharma, RK Khangarot, N Kumar, S Chattopdhyay and KP Misra. Rise in UV and blue emission and reduction of surface roughness due to the presence of Ag and Al in monocrystalline ZnO films grown by sol-gel spin coating. *Mater. Tech.* 2021; **36**, 541-51.

[17] M Dehghan and A Behjat. Deposition of zinc oxide as an electron transport layer in planar perovskite solar cells by spray and SILAR methods comparable with spin coating. *RSC Adv*. 2019; **9**, 20917-24.

[18] P Popielarski, L Mosinska, W Bala, K Paprocki, Yu Zorenko, T Zorenko and M Sypniewska. Persistent photoconductivity in ZnO thin films grown on Si substrate by spin coating method. *Opt. Mater.* 2019; **97**, 109343.

[19] MI Khan, KA Bhatti, R Qindeel, N Alonizan and HS Althobaiti. Characterization of multilayer ZnO thin films deposited by sol-gel spin coating technique. *Results Phys*. 2017; **7**, 651-5.

[20] S Islam, KMA Hussain and MJ Rashid. Deposition and optical characterization of ZnO thin films on glass substrate. *J. Phys. Conf.* 2018; **1086**, 012009.

[21] N Hacini, M Ghamnia, MA Dahamni, A Boukhachem, JJ Pireaux and L Houssiau. Compositional, structural, morphological, and optical properties of ZnO thin films prepared by PECVD technique. *Coatings* 2021; **11**, 202.

[22] W Yang, F Wang, Z Guan, P He, Z Liu, L Hu, M Chen, C Zhang, X He and Y Fu. Comparative study of ZnO thin films grown on quartz glass and sapphire (001) substrates by means of magneton sputtering and high-temperature annealing. *Appl. Sci*. 2019; **9**, 4509.
[23] CY Tsai, JD Lai, SW Feng, CH Chen, FW Yang, HC Wang and LW Tu. Characterizations and growth of textured well-faceted ZnO films by low-pressure chemical vapor deposition on ITO glass substrates. *Superlattice. Microst.* 2017; **111**, 1073-81.
[24] S Arora. ZnO/MgO/ITO structured thin film transistor for ultraviolet photo detector application. *Mater. Today Proc.* 2020; **30**, 150-2.
[25] J Soudi, KM Sandeep, BK Sarojini, PS Patil, SR Maidur and KM Balakrishna. Thermo-optic effects mediated self focusing mechanism and optical power limiting studies of ZnO thin films deposited on ITO coated PET substrates by RF magnetron sputtering under continuous wavelength laser regime. *Optik* 2021; **225**, 165835.
[26] D Aryanto, RM Maulana, T Sudiro, Masturi, AS Wismogroho, P Sebayang, M Ginting and P Marwoto. Effect of post-thermal annealing on the structural of ZnO thin films deposited using sol-gel spin-coating method. *AIP Conf. Proc*. 2017; **1862**, 030045.
[27] D Aryanto, P Marwoto, T Sudiro, AS Wismogroho and Sugianto. Growth of a-axis-oriented Al-doped ZnO thin film on glass substrate using unbalanced DC magnetron sputtering. *J. Phys. Conf.* 2019; **1191**, 012031.
[28] E Muchuweni, TS Sathiaraj and H Nyakotyo. Synthesis and characterization of zinc oxide thin films for optoelectronic applications. *Heliyon* 2017; **3**. e0028.
[29] S Ilyas, Heryanto, B Abdullah, and D Tahir. X-ray diffraction analysis of nanocomposite Fe_3O_4/activated carbon by Williamson-Hall, and size-strain plot methods. *Nano Struct. Nano Objects* 2019; **20**, 100396.
[30] A Katiyar, N Kumar, P Srivastava, RK Shukla and A Srivastava. Structural and physical parameters of sol-gel spin coated ZnO thin films: Effect of sol concentration. *Mater. Today Proc*. 2020; **29**, 1098-103.
[31] SH Sabeeh and RH Jassam. The effect of annealing temperature and Al dopant on characterization of ZnO thin films prepared by sol-gel method. *Results Phys.* 2018; **10**, 212-6.
[32] AT Nomaan, AA Ahmed, NM Ahmed, MI Idris, MR Hashim and M Rashid. ZnO quantum dot based thin films as promising electron transport layer: Influence of surface-to-volume ratio on the photoelectric properties. *Ceram. Int.* 2021; **47**, 12397-409.
[33] J Sun, C Shan, M Zhao and D Jiang. Research on piezo-phototronic effect in ZnO/AZO heterojunction flexible ultraviolet photodetectors. *Optik* 2021; **243**, 167472.
[34] H Ali, AM Alsmadi, B Salameh, M Mathai, M Shatnawi, NMA Hadia and EMM Ibrahim. Influence of nickel doping on the energy band gap, luminescence, and magnetic order of spray deposited nanostructured ZnO thin films. *J. Alloy. Comp.* 2020; **816**, 152538.
[35] U Chaitra, D Kekuda and KM Rao. Effect of annealing temperature on the evolution of structural, microstructural, and optical properties of spin coated ZnO thin films. *Ceram. Int.* 2017; **43**, 7115-22.
[36] AM Alsaada, QM Al-Bataineh, AA Ahmad, Z Albataineh and A Telfah. Optical band gap and refractive index dispersion parameters of boron-doped ZnO thin films: A novel derived mathematical model from the experimental transmission spectra. *Optik* 2020; **211**, 164641.
[37] G Malik, S Mourya, J Jaiswal and R Chandra. Effect of annealing parameters on optoelectronic properties of highly ordered ZnO thin films. *Mater. Sci. Semicond. Process.* 2019; **100**, 200-13.